

## Engineering the ‘Missing Link’ in Biosynthetic (–)-Menthol Production: Bacterial Isopulegone Isomerase

Andrew Currin, Mark S. Dunstan, Linus O. Johannissen, Katherine Anne Hollywood, Maria Vinaixa, Adrian Jervis, Neil Swainston, Nicholas Rattray, John Gardiner, Douglas B Kell, Eriko Takano, Helen S. Toogood, and Nigel S. Scrutton

ACS Catal., **Just Accepted Manuscript** • DOI: 10.1021/acscatal.7b04115 • Publication Date (Web): 24 Jan 2018

Downloaded from <http://pubs.acs.org> on January 24, 2018

### Just Accepted

“Just Accepted” manuscripts have been peer-reviewed and accepted for publication. They are posted online prior to technical editing, formatting for publication and author proofing. The American Chemical Society provides “Just Accepted” as a free service to the research community to expedite the dissemination of scientific material as soon as possible after acceptance. “Just Accepted” manuscripts appear in full in PDF format accompanied by an HTML abstract. “Just Accepted” manuscripts have been fully peer reviewed, but should not be considered the official version of record. They are accessible to all readers and citable by the Digital Object Identifier (DOI®). “Just Accepted” is an optional service offered to authors. Therefore, the “Just Accepted” Web site may not include all articles that will be published in the journal. After a manuscript is technically edited and formatted, it will be removed from the “Just Accepted” Web site and published as an ASAP article. Note that technical editing may introduce minor changes to the manuscript text and/or graphics which could affect content, and all legal disclaimers and ethical guidelines that apply to the journal pertain. ACS cannot be held responsible for errors or consequences arising from the use of information contained in these “Just Accepted” manuscripts.



# Engineering the ‘Missing Link’ in Biosynthetic (–)-Menthol Production: Bacterial Isopulegone Isomerase

Andrew Currin,<sup>†</sup> Mark S. Dunstan,<sup>†</sup> Linus O. Johannissen,<sup>†</sup> Katherine A. Hollywood,<sup>†</sup>  
Maria Vinaixa,<sup>†</sup> Adrian J. Jervis,<sup>†</sup> Neil Swainston,<sup>†</sup> Nicholas J. W. Rattray,<sup>†</sup> John M.  
Gardiner,<sup>†</sup> Douglas B. Kell,<sup>†</sup> Eriko Takano,<sup>†‡</sup> Helen S. Toogood,<sup>‡</sup> and Nigel S.  
Scrutton<sup>†‡\*</sup>

<sup>†</sup>Manchester Centre for Fine and Speciality Chemicals (SYNBIOCHEM) and <sup>‡</sup>School of  
Chemistry, Manchester Institute of Biotechnology, University of Manchester, Manchester M1 7DN,  
United Kingdom

## CORRESPONDING AUTHOR

\*Professor Nigel S. Scrutton, Phone: +44 (0)1613065152. Fax: +44 (0)1613068918. E-mail:  
nigel.scrutton@manchester.ac.uk

## ABSTRACT

The realisation of a synthetic biology approach to microbial (1*R*, 2*S*, 5*R*)-(–)-menthol (**1**) production relies on the identification of a gene encoding an isopulegone isomerase (IPGI), the only enzyme in the *Mentha piperita* biosynthetic pathway as yet unidentified. We demonstrate that  $\Delta$ 5-3-ketosteroid isomerase (KSI) from *Pseudomonas putida* can act as an IPGI, producing (*R*)-(+)-pulegone (*R*)-**2** from (+)-*cis*-isopulegone (**3**). Using a robotics-driven semi-rational design strategy, we identified a key KSI variant encoding four active site mutations, which confer a 4.3-fold increase in activity over the wild-type enzyme. This was assisted by the generation of crystal structures of four KSI variants, combined with molecular modelling of **3** binding to identify key active site residue targets. The KSI variant was demonstrated to function efficiently within cascading biotransformations with downstream *Mentha* enzymes pulegone reductase and (–)-menthone:(–)-menthol reductase to generate **1** from **3**. This study introduces the use of a recombinant IPGI, engineered to function efficiently within a biosynthetic pathway for the production of **1** in microorganisms.

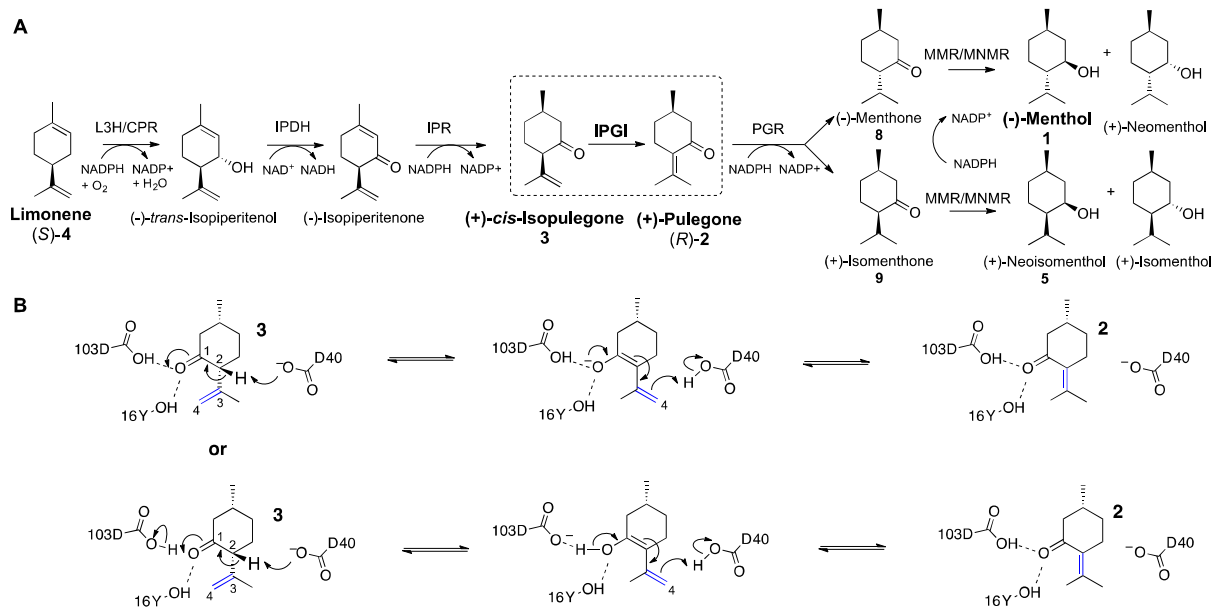
## KEYWORDS

Biosynthetic (–)-menthol production; ketosteroid isomerase; isopulegone isomerase; enzyme engineering; robotics.

## INTRODUCTION

Limonene and its related derivatives are the most abundant, naturally sourced monoterpenoids known.<sup>1</sup> These natural products are commonly used in the perfume, fragrance and flavour industries.<sup>2-3</sup> For example, (*R*)-limonene ((*R*)-**4**) is the major essential oil constituent of orange peels, and is often found in cleaning products.<sup>4</sup> In contrast *Mentha x piperita* (peppermint) generates (*S*)-limonene ((*S*)-**4**), which is subsequently converted into menthol isomers (Scheme 1A).<sup>2,5</sup> The most commercially useful isomer is **1**, known by its characteristic cooling anaesthetic effects and aroma.<sup>6</sup> It also has antibacterial, anticancer and anti-inflammatory activities, making it a valuable natural product.<sup>7-10</sup>

Commercially, **1** is utilised both as a pure compound and as a component of the essential oil of peppermint, with an estimated 30,000 tonnes consumed annually.<sup>11</sup> Whilst the majority of **1** is extracted from *Mentha canadensis*, a large proportion is generated synthetically (US\$ 300 million annually).<sup>12</sup> The two major synthetic routes to **1** are the Haarmann-Reimer route from *m*-cresol and the Takasago synthesis utilising  $\beta$ -pinene.<sup>13</sup> However, the flavour and fragrance industries and/or consumers may demand that these compounds are supplied from natural sources, particularly when used as food additives.



**Scheme 1.** A) The biosynthesis of **1** and (+)-neoisomenthol (**5**) from (*S*)-**4**. Abbreviations: L3H = (*-*)-limonene-3-hydroxylase; IPDH = (*-*)-*trans*-isopiperitenol dehydrogenase; IPR = (*-*)-isopiperitenone reductase; IPGI = (*+*)-*cis*-isopulegone isomerase; PGR = (*+*)-pulegone reductase; MMR = (*-*)-menthone: (*-*)-menthol reductase and MNMR = (*-*)-menthone: (*-*)-neomenthol reductase.<sup>2</sup> B) Proposed KSI catalytic mechanism with **3**, based on the known mechanism of the enzyme towards  $\Delta^5$ -3-ketosteroids.<sup>14</sup>

Naturally sourced peppermint oil can vary in both relative composition of its monoterpene constituents and overall yields due to fluctuating environmental conditions. This leads to price

1 volatility, and increased arable land competition for more profitable crops, such as biofuel biomass  
2 production. Optimisation of peppermint oil production through conventional breeding methods is  
3 difficult as it is a sterile hybrid plant.<sup>2, 15</sup> Additionally purification of **1** from essential oil requires  
4 expensive and low-yielding steam distillation and filtration processes to generate a usable  
5 product.<sup>16-17</sup> Therefore, alternative clean biosynthetic routes to these compounds are a commercially  
6 attractive prospect to generate **1** with a 'natural' label.  
7  
8  
9  
10

11 One alternative 'natural' route is to introduce the biosynthetic pathway of **1** into cost effective and  
12 even food-compatible microorganisms.<sup>18-19</sup> This general synthetic biology approach generates  
13 biological factories, where rapid fine chemicals production can be achieved sustainably using non-  
14 petroleum renewable feedstocks, with a reduced land burden and higher product consistency and  
15 purity.<sup>20-22</sup> Such an approach has proved commercially successful in the semisynthetic industrial-  
16 scale production (*ca.* 35 tonnes per annum) by Sanofi of artemisinin, a major active ingredient in  
17 modern malarial treatments. Similarly, the semisynthetic production of Taxol has been  
18 demonstrated, where microorganism biofactories generated the precursor taxadiene using  
19 introduced pathways.<sup>20</sup>  
20  
21  
22  
23  
24  
25

26 We recently described the incorporation of the *M. piperita*-based biosynthetic pathway from (*R*)-**2**  
27 to **1** into *Escherichia coli*.<sup>23</sup> An *in vitro* protocol was established where **1** was successfully  
28 generated, utilising *E. coli* cell extracts as the biocatalyst source. However, a more cost-effective  
29 route would be an *in vivo* approach, where the full pathways from simple carbon sources to **1** would  
30 be incorporated, and the microorganisms would be grown on waste feedstock. The six enzymatic  
31 steps from (*S*)-**4** to **1** in *Mentha* sp. have been well characterised,<sup>5, 24-30</sup> and the native enzymes for  
32 five of these reactions have been sequenced and functionally expressed in *E. coli* (Scheme 1A).<sup>4-5,</sup>  
33  
34  
35  
36  
37  
38  
39  
40  
41  
42  
43  
44  
45  
46  
47  
48  
49  
50  
51  
52  
53  
54  
55  
56  
57  
58  
59  
60

23, 28, 30-31 The remaining enzyme is isopulegone isomerase (IPGI), which catalyses the double bond  
migrating isomerisation (C3-C4 to C2-C3) of **3** to (*R*)-**2** (Scheme 1A-C).<sup>26</sup> Early studies with  
impure native *Mentha* IPGI identified a 54 kDa protein complex<sup>2, 24</sup> exhibiting cofactor-free  
isomerisation, utilising a mechanism similar to bacterial  $\Delta^5$ -3-ketosteroid isomerases (KSI).<sup>26</sup>  
Therefore, the IPGI mechanism likely involves deprotonation of the C2 $\alpha$  hydrogen of **3** by an  
enzymatic proton acceptor (D40 in KSI), to form an enolate intermediate (Scheme 1B-C), stabilised  
by hydrogen bonding residues (Y16 and D103 in KSI). A proton-donating residue then transfers its  
proton to C4, leading to double bond migration to C2-C3 and reformation of the carbonyl group. As  
no significant ketosteroid isomerase-like proteins have been annotated in plant genomes, the protein  
sequence of native IPGI is likely to remain elusive until the completion of the full annotation of the  
*Mentha longifolia* genome sequence.<sup>32</sup>

To complete the construction of a pathway from (*S*)-**4** to **1** in *E. coli*, we investigated a well-studied bacterial  $\Delta 5$ -3-ketosteroid isomerase from *Pseudomonas putida*,<sup>14, 33-34</sup> and found it exhibited low activity towards **3**. To improve the IPGI activity, we performed three rounds of automated mutagenesis to improve yields of **2**. The crystal structures of four KSI variants were generated, to assist the structure-guided mutagenesis approach to improve the binding of **3** to the enzyme. Molecular dynamics simulations and DFT modeling were applied to the most successful variant, to investigate the mode of increase in activity. The performance of the optimised KSI variant within both *in vitro* and *in vivo* biocatalysis cascades from **3** to **1** was demonstrated. Therefore, the identification and optimisation of a substitute IPGI is a critical step in the future generation of a potentially industrially *E. coli* strain capable of producing ‘natural’ **1**.

## EXPERIMENTAL SECTION

**Design and synthesis of KSI variants.** The wild type gene sequence encoding the  $\Delta 5$ -3-ketosteroid isomerase from *P. putida* (UniProt ID: P07445) was designed using the GeneGenie online tool, containing a C-terminal His<sub>6</sub>-tag.<sup>35</sup> Mutagenic oligonucleotides for the first-generation libraries encoding ambiguous codons for 16 residues were designed optimised for *E. coli* expression using CodonGenie (Tables S1-S2).<sup>36</sup> Eight overlapping DNA oligonucleotides (up to 80 nt in length) were used to assemble the full length genes using the SpeedyGenes gene synthesis method (Supporting Information Section S2.5).<sup>37-38</sup> Purified genes were ligated into linearised pET21b (Novagen) to generate a C-terminally His<sub>6</sub>-tagged enzyme by In-Fusion cloning (Clontech), according to the manufacturers protocol. Cloning products were transformed into T7 Express competent *E. coli* cells and grown on LB agar plates containing 100  $\mu$ g/ml ampicillin, followed by incubation overnight at 37 °C.

The second- and third-generation variants were constructed using asymmetric PCR mutagenesis,<sup>39-40</sup> followed by ligation into linearised pET21b by In-Fusion cloning. These mutations were designed as double or triple variants of the first generation residues identified as providing hits (V88I, L99X and D103S). The final variant was a combination of 4 individual positive mutations (V88I/L99V/V101A/D103S).

**Gene synthesis of *Mentha* biocatalysts.** The protein sequences for the following enzymes from *M. piperita* were obtained from UniProt (<http://www.uniprot.org>): pulegone reductase (MpPGR; Q6WAU0) and (-)-menthone:(-)-menthol reductase (MMR; Q5CAF4). The respective gene sequences were designed and synthesised and subcloned into pET21b by GeneArt (ThermoFisher), incorporating a C-terminal His<sub>6</sub>-tag and applying codon optimisation techniques of rare codon removal for optimal expression in *E. coli*. Each construct was transformed into *E. coli* T7 Express,

1 and grown on LB agar plates containing 100 µg/ml ampicillin, followed by incubation overnight at  
2 37 °C.  
3  
4

5 **Robotics-driven production and purification of variant libraries.** Robotic colony picking and  
6 auto induction media inoculation (Formedium, 100 µg/mL ampicillin) of first generation libraries  
7 was performed into deep well plates (Hamilton Robotics), including replica plating into LB  
8 (Formedium, 100 µg/mL ampicillin) for glycerol stock generation. Plates were covered with a  
9 Breathseal sealer (Greiner Bio-One) and incubated at 30 °C, 1000 rpm for 24 h. Each variant  
10 underwent robotic cell lysis, extraction and purification using Ni-NTA resin (Qiagen; 50 µL per  
11 variant) prior to enzymatic assays (see Supporting Information Section S3.1 for details). Enzyme  
12 concentrations were determined using the Bradford assay (Bio-Rad) following the manufacturers  
13 protocol.  
14  
15  
16  
17  
18  
19

20 **KSI variant biotransformation screen.** Substrate **3** (85% purity) was synthesised by Dr Aisling  
21 Miller (University of Manchester), using a combination of chemical and enzymatic  
22 transformations.<sup>41</sup> Reactions (200 µL) were performed in 50 mM Tris pH 7.0 containing **3** (1 mM)  
23 and KSI extract (189 µL) and incubated at 30 °C for 24 h (180 rpm). Samples were prepared for  
24 GCMS analysis by solvent extraction with 180 µL ethyl acetate containing 0.01% *sec*-butylbenzene  
25 as the internal standard, and dried with anhydrous MgSO<sub>4</sub>. GC-MS achiral quantitative analysis was  
26 conducted on a 7890B GC coupled to a 5975 series MSD quadrupole mass spectrometer and  
27 equipped with a 7693 autosampler (Agilent Technologies). Chiral product analysis was performed  
28 by analysing reactions by GC using an Agilent Technologies 7890A GC system with an FID  
29 detector and a Chirasil-DEX-CB column (Agilent; 25 m, 0.32 mm, 0.25 µm). Further  
30 chromatography details can be found in Supporting Information Section S3.2.  
31  
32  
33  
34  
35  
36  
37

38 Yields of (*R*)-**2** were corrected for the initial concentration present in substrate **3** (15%). Due to  
39 limitations in the quantity of in-house synthesised **3**, three colonies per plate were pooled together  
40 to test for an increase in yield of (*R*)-**2**. Pooled samples exhibiting an increased (*R*)-**2** yield  
41 compared to wild-type KSI were rescreened individually, as above, to identify the well(s)  
42 responsible for the improved yield. Quantification was performed by comparing the peak areas to  
43 the calibration curves of authentic standards. Vendor binary files were converted to open mzXML  
44 data format<sup>42</sup> using ProteoWizard msConvert.<sup>43</sup> Automated peak profiling and quantification was  
45 conducted using in-house scripts written in R.  
46  
47  
48  
49  
50

51 **Comparative activity of the variants.** First generation KSI variant hits and later mutants generated  
52 by site-specific mutagenesis were cultured from glycerol stocks in LB medium containing 100  
53 µg/mL ampicillin as above. The KSI-encoding plasmids were extracted and purified (Macherey-  
54 Nagel), and underwent Sanger sequencing to identify the mutation present. Larger scale cultures  
55  
56  
57  
58  
59  
60

1 (500 mL) were generated for each variant in the same antibiotic-selective LB medium, and  
2 incubated at 37 °C (180 rpm) to an OD<sub>600nm</sub> of 0.6-0.8, followed by induction with 0.1 mM  
3 isopropyl-β-D-thiogalactopyranoside (IPTG). Cultures were incubated overnight at 25 °C (180 rpm)  
4 and the cells harvested by centrifugation (3000 x g for 5 min). Each variant underwent extraction (4  
5 mL lysis buffer) and purification (0.5 mL Ni-NTA resin) using the same protocol and buffers as in  
6 the initial screen (Supporting Information Section S3.1). Biotransformations were performed with 1  
7 mM **3** as above (10 μM KSI), and the variants that did not display improved yield of (*R*)-**2** above  
8 wild type (false positives) were discarded.

9  
10  
11  
12  
13  
14  
15 **Steady-state reactions with (+)-*cis*-isopulegone.** Continuous steady state-reactions with **3** were  
16 performed with selected purified variants to investigate the effect of the mutation(s) on the reaction  
17 rate. Reactions (100 μL) were composed of 50 mM Tris pH 7.0 containing 1 mM **3** within UV-Star  
18 microplates (Greiner Bio-One) and covered with a ClearVue sealing sheet. Product formation was  
19 detected by monitoring the absorbance at 260 nm for 1 h at 20 °C using a CLARIOstar microplate  
20 reader (BMG Labtech). Concentrations were determined by comparison to a standard curve (Figure  
21 S1), and data were corrected for both **3** and (*R*)-**2** loss over 1 h (control substrate and product data).

22  
23  
24  
25  
26  
27 **Cascade biocatalysis.** The *Mentha* enzymes MpPGR and MMR were produced (500 mL culture;  
28 20 °C) and purified according to the method for the KSI variants (Supporting Information Section  
29 S3.1). Reactions (200 μL) were performed in 50 mM Tris pH 7.0 containing 10 μM KSI, 1 μM  
30 MpPGR, 0.3 μM MMR, 1 mM **3** and a cofactor recycling system (10 U Sigma glucose  
31 dehydrogenase, 10 μM NADP<sup>+</sup> and 15 mM D-glucose) to supply MpPGR and MMR with  
32 NADPH.<sup>23</sup> Reactions were incubated at 30 °C for 24 h (180 rpm), and the extracts were analysed by  
33 GC-MS as before.

34  
35  
36  
37  
38 **Pathway assembly and *in vitro* activity.** The genes encoding KSI variant V88I/L99V/V101A/  
39 D103S, MpPGR and MMR and their respective ribosomal binding sequences (RBS) were amplified  
40 by PCR and ligated into pET21b using In-Fusion cloning to create an expression construct under  
41 the control of one T7 promoter. The RBS of MMR was modified by PCR mutagenesis to generate  
42 three constructs with lower predicted translation initiation rates (Table S3). Each construct was  
43 transformed into competent *E. coli* NEB5α cells, and underwent culture growth, plasmid  
44 purification and DNA sequencing as before.

45  
46  
47  
48  
49  
50 The plasmids were transformed into competent *E. coli* NiCo21 (DE3) expression cells and cultured  
51 on LB agar containing 100 μg/mL ampicillin. Single colonies were selected and grown in 200 mL  
52 phosphate buffered Terrific Broth pH 7.0 containing 0.4% glycerol and 100 μg/mL ampicillin,  
53 followed by induction with 0.1 mM IPTG. The cultures were incubated overnight at 20 °C, and  
54 harvested by centrifugation (3000 x g). Soluble cell extracts were generated using lysis buffer (3  
55  
56  
57  
58  
59  
60

1 mL pH 7.0), sonication and centrifugation as above. Cascade biocatalysis reactions were set up as before, except the purified enzymes were replaced with 50  $\mu$ L of cell extract.

**Protein crystallization and structure solution.** Purified KSI variants D103S, V88I/L99V, V88I/L99V/D103S and V88I/L99V/V101A/D103S (10 mg/mL) were crystallised using a Mosquito robot (TTP Labtech) and the following crystallisation solutions: *i*) 10-25% PEG3350 with 0.2 M  $MgCl_2$ ; *ii*) 10-25% PEG3350 with 0.2 M ammonium acetate (pH 4.6) and *iii*) 10-25% PEG3350 with 0.2 M ammonium acetate (pH 5.5). Crystals were flash frozen in 30 % glycerol and data collected at the Diamond light source (beamlines IO4 and IO3). Reflections were merged and scaled with Xia2.<sup>44</sup> All mutant structures were solved by molecular replacement using Phaser-MR (CCP4)<sup>45</sup> and wild type KSI (PDB code: 1OPY) as a search model. Initial model building was done with AutoBuild (PHENIX)<sup>46</sup> followed by iterative cycles of manual model building and refinement in COOT<sup>47</sup> and Phenix.refine<sup>48</sup> respectively. Mutations could be clearly identified in *Fo-Fc* difference maps and were modeled accordingly. The final data collection and refinement statistics are found in Table S4. The atomic coordinates and structure factors (6F4Y, 6F50, 6F53 and 6F54) have been deposited in the Protein Data Bank, Research Collaboratory for Structural Bioinformatics, Rutgers University, New Brunswick, NJ (<http://www.rcsb.org/>).

**Molecular modelling.** DFT modelling was performed using Gaussian09 revision D.01.<sup>49</sup> An active site model was created from the crystal structure of KSI with bound androstenedione (**6**; PDB ID 1OHS) including the side-chains and  $\alpha$ -carbons of the 15 first-shell residues shown in Figure S4, with substrate **3** built in using the coordinates of the corresponding ligand **6** atoms as the starting point. Energy minimisation was carried out using the B3LYP hybrid functional and 6-31G(d) basis sets<sup>50</sup> with the D3 version of Grimme's dispersion.<sup>51</sup> Since the active site is solvent exposed, a continuum solvent model was used to mimic the shielding effect of water. Molecular dynamics simulations were carried out using Gromacs 4.6.1 with the Gromos 53A6 force field and periodic boundary conditions.<sup>52-53</sup> For WT KSI, the crystal structure of KSI with bound **6** (PDB: 1OHS) was used, with substrate **3** built in using the coordinates of the corresponding ligand **6** atoms as the starting point. For KSI variant V88I/L99V/V101A/D103S, ligand **3** was placed in the active site of the crystal structure (PDB: 1OPY) by aligning the protein to the wild type KSI model. The energy minimization parameters are described in detail in Supporting Information Section S6.

## RESULTS AND DISCUSSION

**Identification of KSI as a (+)-*cis*-isopulegone isomerase.** Prior studies with the partially purified native *M. piperita* isomerase suggested its mechanism resembled that of the bacterial  $\Delta 5$ -3-ketosteroid isomerase family (EC 5.3.3.1).<sup>26</sup> These enzymes catalyze the isomerization of  $\Delta 5$ -3-

1 ketosteroids, such as 5(10)estrene-3,17-dione, to the equivalent  $\Delta^4$ -3-ketosteroid by intramolecular  
2 transfer of the C4 $\beta$  proton to the C6 $\beta$  position.<sup>54</sup> Prior studies showed that KSI from *P. putida* reacts  
3 with truncated substrate 3-cyclohexen-1-one, forming the more stable 2-cyclohexen-1-one.<sup>55</sup>  
4 Therefore we postulated that KSI might react with the structurally related compound **3** to generate  
5 (*R*)-**2** using a similar mechanism (Scheme 1B).  
6  
7  
8  
9

10 A C-terminally His<sub>6</sub>-tagged version of wild-type KSI from *P. putida* was generated, and  
11 biotransformations with **3** showed **2** was formed (35% yield). Chiral GC analysis confirmed the  
12 product generated was (*R*)-**2**, the enantiomeric form required for **1** biosynthesis (Table S5).<sup>2</sup> An  
13 additional minor quantity (<1% yield) of side product (-)-*trans*-isopulegone (**7**) was also detected.  
14 As the (*R*)-**2** yields were judged to be too low for biotechnological applications, we employed a  
15 directed evolution strategy to engineer KSI for improved synthesis of (*R*)-**2**.  
16  
17  
18  
19

20 **High throughput directed evolution of KSI.** Comparative studies of KSI with single and multiple  
21 ring substrates showed that while the specificity ( $k_{cat}/K_m$ ) is 27,000 fold higher for steroid  
22 substrates, the reaction rates were within two-fold.<sup>55</sup> This suggests that remote binding interactions  
23 with steroid substrates have a marked impact on the strength of substrate binding, and single-ring  
24 substrates like **3** may have poor binding affinity. Therefore, our initial KSI mutagenesis strategy  
25 was to increase binding of **3** by targeting every amino acid known or predicted to interact with  
26 steroid substrates. An examination of the co-crystal structure of wild-type KSI bound to the reaction  
27 intermediate analogue equilenin (PDB 1OH0)<sup>34</sup> showed that sixteen residues were located within 5  
28 Å of the ligand. Given the overall apolar nature of the KSI active site and **3**, maintaining this  
29 environment would likely maximise our search for optimised mutations whilst minimising the size  
30 of the variant libraries and subsequent screening effort. Reducing the number of screening assays  
31 was critical given the limited availability of the in-house synthesised substrate **3**.  
32  
33  
34  
35  
36  
37  
38  
39

40 Twelve of these residues were targeted for individual limited randomizing mutagenesis, where the  
41 general physicochemical properties of the amino acids were conserved (Table S1). Residues Y16  
42 and Y57 are both known to partake in H-bonding with the substrate carbonyl moiety, therefore  
43 these residues were mutated combinatorially, using an ambiguous codon (WVC) that encodes other  
44 residues capable of H-bonding. Similarly, residues V88 and L99 were selected for combinatorial  
45 mutations using an ambiguous codon (DTK) for hydrophobic residues, given their close proximity  
46 to the substrate analogue.<sup>34</sup> Variant sequences were created by gene synthesis using ambiguous  
47 codons (Table S2) and constructed using the SpeedyGenes protocols.<sup>37-38</sup> In total, 158 variants were  
48 created and screened for improvement in (*R*)-**2** production using high throughput robotic culturing  
49 and protein purification protocols (summarized in Figure S2). Comparative biotransformations were  
50  
51  
52  
53  
54  
55  
56  
57  
58  
59  
60

performed with **3**, with quantitation and product identification by GC-MS, to identify variants with higher activity than wild type KSI.

**Table 1.** Biotransformations of wild type and variant KSI with **3**.

Round	Variant	Specific Activity ( $\mu\text{M}/\mu\text{M}/\text{d}$ ) <sup>a</sup>	Relative Activity (fold)
-	Wild type	13.88 $\pm$ 0.08	1.0
1	D103S	20.09 $\pm$ 1.16	1.4
	L99I	23.58 $\pm$ 0.10	1.7
	L99V	18.46 $\pm$ 0.48	1.3
	V88I/L99V	19.39 $\pm$ 0.57	1.4
2	V88I/L99V/D103S	26.47 $\pm$ 1.59	1.9
	L99V/D103S	25.51 $\pm$ 0.83	1.8
	L99I/D103S	25.91 $\pm$ 0.58	1.9
3	V88I/L99V/V101A/D103S	63.10 $\pm$ 0.61	4.5

Duplicate reactions (200  $\mu\text{L}$ ) were performed in 50 mM Tris pH 7.0 containing 1 mM **3** and 10  $\mu\text{M}$  KSI. After a 24 h incubation at 30  $^{\circ}\text{C}$  (180 rpm), reactions were extracted with 180  $\mu\text{L}$  ethyl acetate containing 0.01% *sec*-butylbenzene and dried with anhydrous  $\text{MgSO}_4$ . Products were analysed by GC-MS using a DB-WAX column.

<sup>a</sup>Specific activity is expressed as  $\mu\text{M}$  (*R*)-**2** produced per  $\mu\text{M}$  KSI in 24 hours.

Four enzyme variants were identified as having minor increases in (*R*)-**2** yield (1.4-1.7 fold), three of which contained mutations of residue L99 (L99I, L99V and V88I/L99V; Table 1). Interestingly, both L99I and L99V involve mutations to a smaller side chain, suggesting these changes may impact on **3** binding by reducing steric hindrance. The fourth improved variant D103S also contained a smaller side chain, however there was also a change from a negatively charged moiety to a polar functionality. As a serine hydroxyl group can participate in H-bonding, this mutation might maintain the native enzyme hydrogen bonding interaction with the substrate carbonyl group.

**Second round: compiling mutations.** To investigate the combinatorial effect of the initial screen variants, the L99X-containing single and double mutants were each combined with D103S using asymmetric PCR mutagenesis.<sup>39-40</sup> Each variant was purified and underwent biotransformations to determine any improvement in (*R*)-**2** yield by GC-MS (Table 1). Unfortunately, these double and triple variants showed only moderate improvements in (*R*)-**2** yield compared to wild type enzyme (1.8-1.9 fold).

**Third round: Structure-guided mutation.** To ensure the mutations in the active site and surrounding residues did not affect the overall fold of KSI, we solved the X-ray crystal structures of four key variants D103S, V88I/L99V, V88I/L99V/D103S and V88I/L99V/V101A/D103S (Table S4). Each of these structures showed backbone conformations virtually identical to the co-crystal structure of wild-type KSI bound to reaction intermediate analogue equilenin (Figure S3),<sup>34</sup> with RMSD values of 0.427, 0.418, 0.443 and 0.357, respectively. All the mutations could be clearly identified in *Fo-Fc* difference maps, and were incorporated without any major displacement of the

backbone atoms or surrounding residues. We did note minor rearrangements of backbone atoms within the loop region 90-98 (results not shown). This loop is exposed to the bulk solvent and shows above average B factors compared to surrounding residues, implying the observed differences are down to inherently flexibility, rather than any mutational changes to neighbouring residues.

Inspecting the spatial arrangement of these mutations showed residue V101 was positioned directly between L99V and D103S, highlighting it as another potential target for mutagenesis (Figure 1B inset). Given that most of the existing variants resulted in a shortening of the amino acid side chain, the triple variant was modified to incorporate the mutation V101A. Biotransformations were performed on the KSI V88I/L99V/V101A/D103S variant, which showed a more dramatic increase in (*R*)-**2** production over wild type enzyme (4.5-fold; Table 1). Therefore, the modification of V101 to an alanine residue has resulted in over a 2-fold increase in (*R*)-**2** formation over the triple variant.

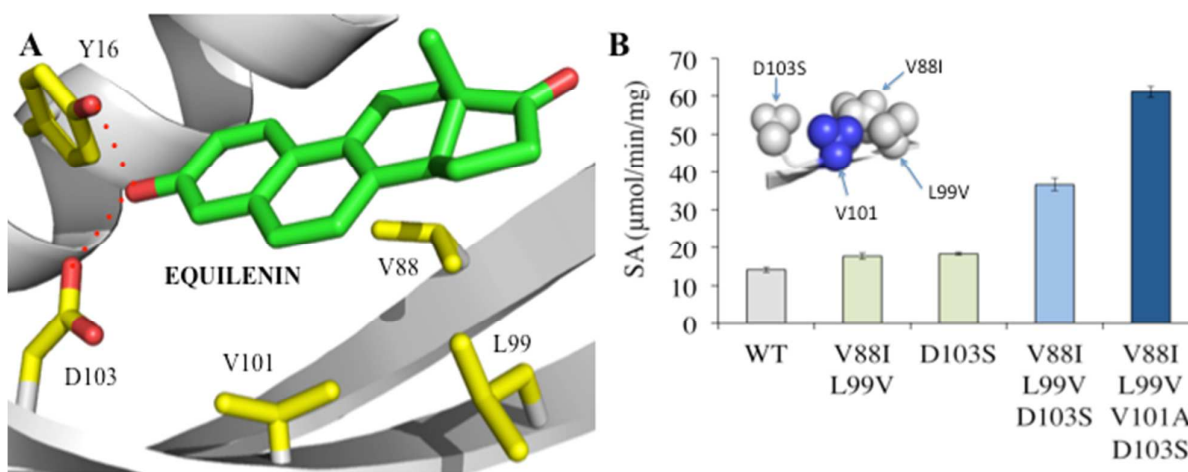


**Figure 1.** Location of key active site mutations implicated in improving KSI activity towards **3**. A) Residues located in the equilenin-binding region of wild type KSI from *P. putida* (PDB: 1OH0).<sup>34</sup> The residues and equilenin are shown as atom coloured sticks with yellow and green carbons, respectively. Interactions are shown as red dotted lines. The backbone is shown as a grey cartoon. B) Comparative steady state activity of wild type and variant KSI enzymes. Reactions (100  $\mu\text{L}$ ) were composed of 50 mM Tris pH 7.0 containing 1 mM **3**. The absorbance was monitored at 260 nm for 1 h at 20  $^{\circ}\text{C}$ . Inset: The location of the variant residues in KSI V88I/L99V/D103S. Backbone and mutations are shown as grey ribbons and balls, respectively (blue balls for V101).

To investigate the impact of the mutations further, the specific activity of the variants with substrate **3** was determined under pseudo-steady state conditions (1 h reactions). This method takes advantage of the enolization of **3** to (*R*)-**2**, which results in the development of a peak around 260 nm (Figure S1). First generation variants showed minor rate increases (around 1.3-fold), while a near 2-fold improvement was seen with triple variant V88I/L99V/D103S (Figure 1B). The addition

of mutation V101A generated a 4.3-fold increase in specific activity compared to the WT (61.17  $\mu\text{mol}/\text{min}/\text{mg}$  compared to 14.16  $\mu\text{mol}/\text{min}/\text{mg}$ ; Figure 1B). Therefore, the increases in the overall reaction rate mirror the increased product yields detected in the 24 h biotransformations.

**Modeling and molecular dynamics simulations for KSI variants.** We performed comparative DFT modeling and MD simulations between wild type KSI and variant V88I/L99V/V101A/D103S to investigate the origin(s) of activity rate changes. The DFT optimized model for wild type KSI suggests substrate **3** carbonyl group hydrogen bonds with D103 ( $< 2.0 \text{ \AA}$ ), but the orientation is non-ideal for catalysis due to a less favourable interaction distance for the proton abstraction step (Figure 2 and Figure S4; Scheme 1B). Additionally, residue L99 has reoriented outwards from the active site, causing a twist in the  $\beta$ -hairpin from residue 88 to 99 (Figure S2).

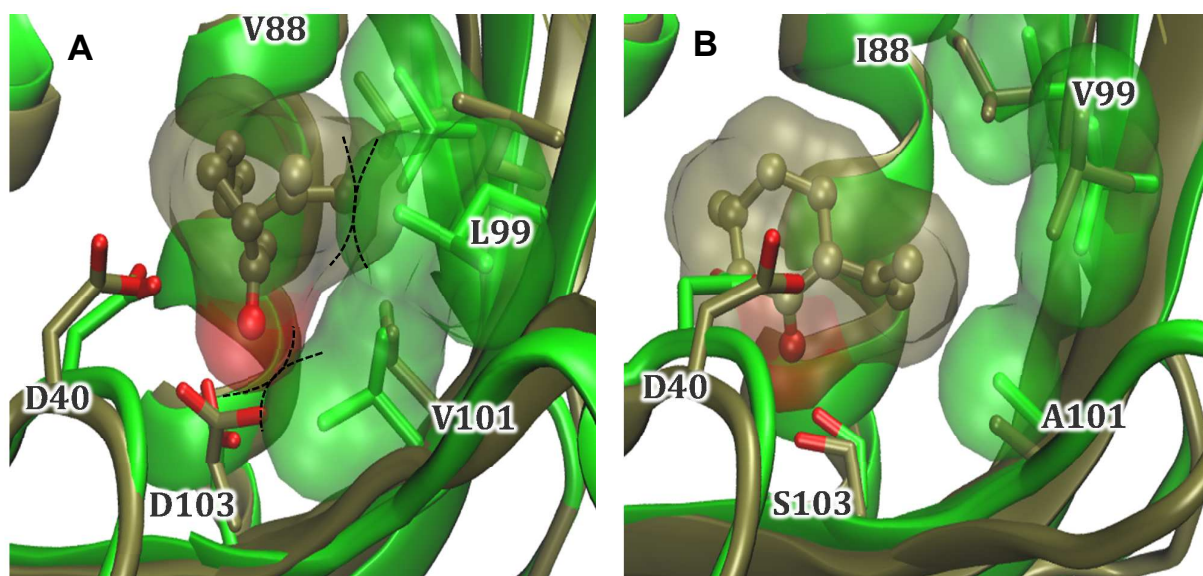


**Figure 2.** Overlay of energy minimised structure (green) and representative structure from MD simulations (brown) for (A) wild-type KSI and (B) variant V88I/L99V/V101A/D103S modelled with **3** in the active site. The solvent accessible surface areas for the substrate and residues 88, 99 and 101 from the representative and minimised structures, respectively, are shown as transparent surfaces. The dotted lines illustrate potential steric clashes between the substrate and enzyme. The MD simulations were performed using Gaussian09 revision D.01.<sup>49</sup>

MD simulations of variant KSI with **3** restrained in a reactive conformation suggests the decrease in bulk of variant residues I88, V99 and A101 allows the substrate to comfortably adopt this position (Figure 2B). The position of **3** looks more ideal, with a D40-substrate hydrogen-oxygen distance of 2.04  $\text{\AA}$  in the DFT model. Therefore, the decrease in bulk of variant residues I88, V99 and A101 has allowed this reorienting of the substrate, whilst still maintaining a (slightly longer) hydrogen bonding interaction with residue S103 (D103 in wild type). MD simulations with the variant model showed no repositioning of the hairpin loop from 88-99 was necessary, as **3** fitted more easily within the active site. Overall, molecular simulations suggest these four mutations have improved

binding of **3** in a functional conformation within the active site. Therefore, the V88I/L99V/V101A/D103S variant was selected for further studies to see if it can be used in cascading reactions for the biosynthetic production of **1** from **3**.

**One-pot (-)-menthol production with purified enzymes.** Initial cascading reactions were performed with purified enzymes to eliminate any interference from competing *E. coli* enzymes present in whole cells and cell extracts (Table 2). Interestingly, reactions with KSI variant V88I/L99V/V101A/D103S showed the formation of ~ 10% of by products, such as *trans*-isopulegone (**7**). This suggests the presence of the 4 mutations has altered the range of possible binding conformations of **3**, leading to additional isomer formation. The pathway from **3** to **1** also requires the presence of two *Mentha* enzymes, namely pulegone reductase (MpPGR)<sup>29</sup> and (-)-menthone:(-)-menthol reductase (MMR) to generate (-)-menthone (**8**) and **1**, respectively (Scheme 1A).<sup>2</sup> Initial biotransformations of purified MpPGR with (*R*)-**2** showed it produced near equivalent yields of **8** and (+)-isomenthone (**9**) (ratio 49:51; Table 2). This differs slightly from previous studies of a non-His<sub>6</sub>-tagged recombinant form of MpPGR, which showed a **8** to **9** ratio of 55:45.<sup>29</sup> However this enzyme showed a significantly higher yield of **8** than seen with the homologous enzyme from *Nicotiana tabacum* (NtDBR) performed under the same reaction conditions.<sup>56</sup> Similarly, purified MMR-His<sub>6</sub> demonstrated similar activity towards **8** as in previous studies,<sup>5</sup> showing primarily **1** production (Table 2).

**Table 2.** Biotransformations of individual enzymes and cascading reactions with *Mentha* monoterpenoids.

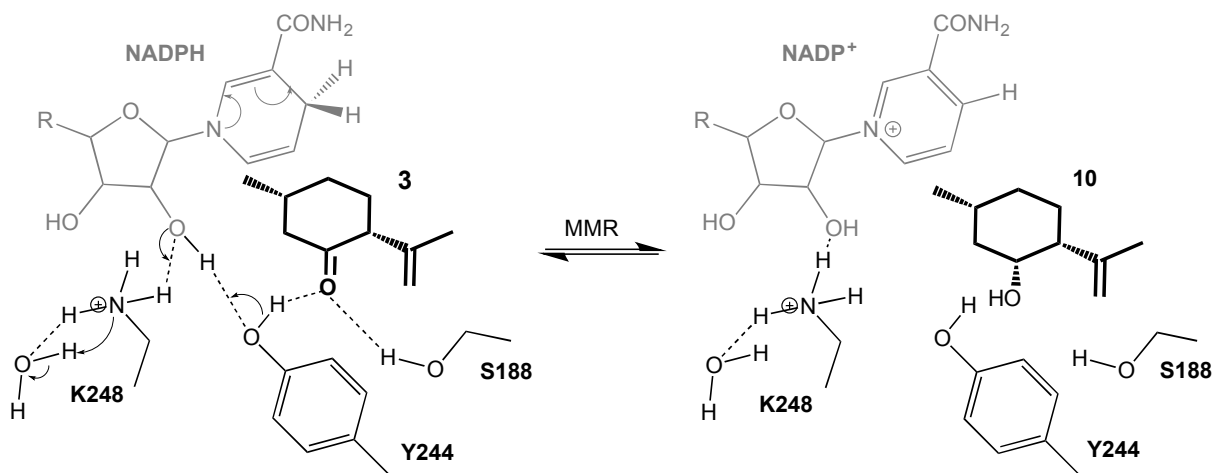
Biocatalyst	Substrate remaining/Product yield (μM)					
	<b>3</b>	( <i>R</i> )- <b>2</b>	<b>8</b>	<b>9</b>	<b>3</b>	<b>5</b>
<i>Individual enzymes</i>						
KSI WT	<b>361.7</b> ± 11.5	210.4 ± 6.0	N/A	N/A	N/A	N/A
KSI variant <sup>a-b</sup>	<b>40.7</b> ± 0.7	436.3 ± 10.8	N/A	N/A	N/A	N/A
MpPGR	N/A	<b>10.0</b> ± 1.1	153.3 ± 5.8	160.1 ± 4.5	N/A	N/A
MMR	N/A	N/A	<b>8.0</b> ± 2.0	N/A	280.7 ± 10.3	N/A
<i>Cascading reactions</i>						
Cascade <sup>b</sup>	<b>16.7</b> ± 1.2	10.3 ± 0.1	25.2 ± 0.9	16.6 ± 0.5	63.4 ± 3.8	11.1 ± 0.6
Cell extract <sup>b</sup>	<b>17.1</b> ± 0.1	11.5 ± 0.5	60.6 ± 1.9	34.8 ± 0.3	52.8 ± 0.9	18.6 ± 0.8
Whole cells <sup>b</sup>	<b>32.5</b> ± 6.7	1.0 ± 2.1	44.7 ± 10.3	98.6 ± 2.4	158.8 ± 0.4	19.6 ± 0.1

Duplicate reactions (200 μL) were performed in 50 mM Tris pH 7.0 containing 1 mM monoterpenoid substrate, enzyme(s) and cofactor recycling system (10 U Sigma glucose dehydrogenase, 10 μM NADP<sup>+</sup> and 15 mM D-glucose). After a 24 h incubation at 30 °C (180 rpm), reactions were extracted with 180 μL ethyl acetate containing 0.01% *sec*-butylbenzene and dried with anhydrous MgSO<sub>4</sub>. Products were analysed by GC-MS using a DB-WAX column (Figure S7). Reactions with individual enzymes had enzyme concentrations of 10 μM. The *in vitro* cascading reaction had enzyme concentrations of 10, 2 and 0.3 μM for KSI variant, MpPGR and MMR, respectively. Control biotransformations of each compound in the absence of enzymes (data not shown) showed losses occurred over 24 h due to non-enzymatic degradation. Therefore the product yields are likely an underestimation of the true yields. The cell extract and whole cell slurry volumes in the cascading reactions were 50 μL. <sup>a</sup>KSI variant = V88I/L99V/V101A/D103S; <sup>b</sup>Additional products were detected that were not quantified (e.g. **7** and (+)-neoisopulegol (**10**)). Substrates are shown in bold. N/A = not applicable.

Initial cascading biotransformations of purified KSI wild-type and variant V88I/L99V/V101A/D103S with MpPGR and MMR with **3** showed the major product was an

isomer of isopulegol (results not shown). Chiral GC analysis of the reaction showed the main isomer formed was (+)-neoiso-isopulegol (**10**), with a minor proportion of (-)-isopulegol generated (Figure S6).<sup>57</sup> However product **1** was also detected, with 5.1-fold higher yields obtained for reactions containing V88I/L99V/V101A/D103S variant KSI (46  $\mu$ M vs 9  $\mu$ M).

Subsequent reactions with each individually purified biocatalyst showed this side product was obtained by the action of MMR on **3**, which differs from earlier studies.<sup>5</sup> However, this apparent disparity is likely due to the 144-fold reduction in the reaction time of the earlier study compared to this work (6-9 min vs 24 h).<sup>5</sup> It is likely that the mechanism of action of MMR with **3** proceeds in a similar manner to the Short Chain Dehydrogenase/Reductase ketoreduction mechanism described previously for MMR and MNMR with substrates **8** and **9** (Scheme 2).<sup>58</sup> Unfortunately, the formation of **10** by MMR appeared to dominate over the reaction with **8**, likely due to the lack of the latter substrate at the start of the reaction.



**Scheme 2.** Proposed mechanism of action of the NADPH-dependent MMR-catalysed reduction of **3** to **10**. This is adapted from the proposed SDR ketoreductase mechanism of MNMR with **8**.<sup>58</sup>

Subsequent cascading reactions were performed with a 30-fold molar excess of KSI over MMR, to allow KSI activity with **3** to predominate. Using this approach, we dramatically increased **1** titres (63.4  $\mu$ M; 14.1% conversion; Table 2) relative to **10**, producing a near 1:1 ratio of products. In addition, a surprising yet advantageous observation was that relatively lower levels of **9** (and subsequently **5**) were produced than expected for MMR, with a combined ratio of 76:24 (**8+1**: **9+5**). Therefore, these studies have demonstrated that KSI variant V88I/L99V/V101A/D103S can be utilised in cascading reactions as the first step in generating **1** from **3**.

**Cascading production of **3** using cell-free extracts and whole cells.** We have previously reported the biosynthesis of menthol isomers from (*R*)-**2**, using *E. coli* cell extracts expressing the enzymes NtDBR and MMR.<sup>23</sup> To further extend this approach; we developed a single expression construct in

1 pET21b containing KSI variant V88I/L99V/V101A/D103S, MpPGR and MMR, with each gene  
2 under the control of one T7 promoter (Table S3). This enabled the IPTG-dependent co-expression  
3 of all three genes in *E. coli*. Biotransformations were performed using cell extracts with **3** in the  
4 presence of a cofactor recycling system, the latter to supply MpPGR and MMR with NADPH. As  
5 expected, the major product obtained was **10**, due to the promiscuous activity of MMR (results not  
6 shown).  
7  
8  
9  
10

11 To mimic the effect of increasing the KSI:MMR concentration ratio *in vivo*, we modified the RBS  
12 sequence upstream of MMR to three alternative ones, each with predicted translation initiation rates  
13 (TIR) less than the existing one of 4100 (1000, 500 and 200; Table S3).<sup>59-60</sup> Of the three constructs,  
14 only the one containing an RBS with a predicted TIR of 500 showed any MMR activity, leading to  
15 the production of both **1** and **10** (Table 2). Cell extracts of this construct yielded 53  $\mu\text{M}$  of **1**, similar  
16 to that obtained with the purified enzyme one-pot biotransformations. The higher levels of **8** and **9**  
17 detected reflects the lower *in vivo* concentration of MMR within this construct. Reactions were also  
18 conducted with whole cells, producing nearly 3-fold higher levels of **1** than cell extract  
19 biotransformations (159  $\mu\text{M}$ , 27% total yield; Table 2) with proportionally less **10**.  
20  
21  
22  
23  
24  
25  
26

27 These studies have demonstrated that these three enzymes have great potential in an overall strategy  
28 for *in vivo* production of **1** in *E. coli*. Ideally KSI V88I/L99V/V101A/D103S would be incorporated  
29 into an *E. coli* construct containing all the remaining enzymes required for **1** production from (*S*)-4  
30 (Scheme 1A). This would enable one-pot biotransformations or *in vivo* fermentations to be  
31 performed using the inexpensive and renewable starting material (*S*)-4. Ultimately, the inclusion of  
32 an (*S*)-4 production pathway would enable *E. coli* to produce **1** *in vivo* from simple sugars.<sup>61</sup> This  
33 would avoid the addition of high concentrations of toxic monoterpene precursors and eliminate  
34 the need for exogenous cofactor recycling systems. Additionally, the low *in vivo* concentration of **3**  
35 would likely minimise pathway hijacking to form **10**, increasing the overall yields of **1**.  
36  
37  
38  
39  
40  
41  
42

## 43 CONCLUDING REMARKS

44 The implementation of a synthetic biology approach to microbial **1** production has been hampered  
45 by the absence of the sequence for the native *Mentha* pathway enzyme IPGI, and the lack of  
46 identification of plant proteins exhibiting homology to bacterial  $\Delta 5$ -3-ketosteroid isomerases known  
47 to catalyze this reaction on steroid substrates. We took the approach of engineering an existing  
48 bacterial  $\Delta 5$ -3-ketosteroid isomerase to improve its activity towards **3**, using a structure-modeling  
49 guided, semi-rational design to identify target residues. Our implementation of a robotics platform  
50 to ensure rapid and reproducible automated gene assembly, enzyme purification and micro-scale  
51 biotransformation screening enabled the identification of potential variant biocatalysts with limited  
52  
53  
54  
55  
56  
57  
58  
59  
60

1 substrate availability. The incorporation of four targeted mutations into KSI enabled a 4.3-fold  
2 increase in IPGI activity, generating a biotechnologically useful enzyme with significant *in vivo*  
3 activity. Further engineering studies could potentially improve its functionality, thereby driving the  
4 cascading reactions towards more efficient **1** production.  
5  
6  
7

8 This is the first report of a non-*Mentha* enzyme with IPGI activity, thereby identifying the ‘missing  
9 link’ to complete the enzymatic route from (S)-**4** to **1**. This will enable for the first time the full  
10 construction of a biosynthetic pathway for microbial production of **1**. The demonstration of  
11 successful **1** production from **3** by engineered *E. coli* adds to a growing number of studies  
12 highlighting the potential usefulness of microbial hosts in monoterpenoid production. It is  
13 anticipated that integrating our existing KSI-MpPGR-MMR construct into a larger chassis will  
14 enable the production of menthol isomers from inexpensive precursors, providing a sustainable and  
15 renewable production platform to meet the growing global demand for natural menthol products.  
16  
17  
18  
19  
20  
21

## 22 ASSOCIATED CONTENT

### 23 Supporting Information

24 The Supporting Information document contains additional experimental details, materials used,  
25 additional tables and figures, results, GC/MS analyses, and discussion of computational and  
26 crystallographic studies. The Supporting Information is available free of charge on the ACS  
27 Publications website at DOI:  
28  
29  
30  
31  
32

### 33 AUTHOR INFORMATION

#### 34 ORCID

35 Andrew Currin: 0000-0001-7845-8837; Linus O. Johannissen: 0000-0002-0916-9094; Maria  
36 Vinaixa: 0000-0001-9804-0171; Neil Swainston: 0000-0001-7020-1236; Nicholas Rattray: 0000-  
37 0002-3528-6905; John M. Gardiner: 0000-0003-1827-6817; Douglas B. Kell: 0000-0001-5838-  
38 7963; Eriko Takano: 0000-0002-6791-3256; Helen S. Toogood: 0000-0003-4797-0293; Nigel S.  
39 Scrutton: 0000-0002-4182-3500  
40  
41  
42  
43  
44

#### 45 Author Contributions

46 We thank Colin Levy for protein crystallisation and data collection, and the wider SYNBIOCHEM  
47 team for their contributions. The manuscript was written through contributions of all authors. All  
48 authors have given approval to the final version of the manuscript.  
49  
50  
51

#### 52 Funding Sources

53 The UK Catalysis Hub (<http://www.ukcatalysishub.co.uk>) is kindly thanked for resources and  
54 support. Funding was provided by the Biotechnology and Biological Sciences Research Council  
55  
56  
57  
58  
59  
60

(BBSRC) and Engineering and Physical Sciences Research Council (EPSRC) under grants BB/M017702/1 (SYNBIOCHEM), BB/J015512/1 and BB/M017702/1.

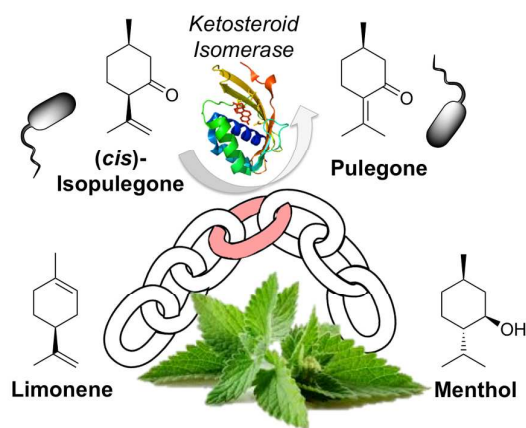
## Notes

AC, HT and NS are named inventors on a submitted patent describing the work in this manuscript.

## ACKNOWLEDGMENTS

The authors would like to acknowledge the assistance given by IT Services and the use of the Computational Shared Facility at The University of Manchester.

## TOC



Bacterial ketosteroid isomerase replaces peppermint isopulegone isomerase for (-)-menthol biosynthesis in *Escherichia coli*.

## REFERENCES

- (1) Duetz, W. A.; Bouwmeester, H.; van Beilen, J. B.; Witholt, B., *Appl. Microbiol. Biotechnol.* **2003**, *61*, 269-277.
- (2) Croteau, R. B.; Davis, E. M.; Ringer, K. L.; Wildung, M. R., *Naturwissenschaften* **2005**, *92*, 562-577.
- (3) Leavell, M. D.; McPhee, D. J.; Paddon, C. J., *Curr. Opin. Biotechnol.* **2016**, *37*, 114-119.
- (4) Alonso-Gutierrez, J.; Chan, R.; Batth, T. S.; Adams, P. D.; Keasling, J. D.; Petzold, C. J.; Lee, T. S., *Metab. Eng.* **2013**, *19*, 33-41.
- (5) Davis, E. M.; Ringer, K. L.; McConkey, M. E.; Croteau, R., *Plant Physiol.* **2005**, *137*, 873-881.
- (6) Watt, E. E.; Betts, B. A.; Kotey, F. O.; Humbert, D. J.; Griffith, T. N.; Kelly, E. W.; Veneskey, K. C.; Gill, N.; Rowan, K. C.; Jenkins, A.; Hall, A. C., *Eur. J. Pharmacol.* **2008**, *590*, 120-126.

- 1 (7) Freires, I. A.; Denny, C.; Benso, B.; de Alencar, S. M.; Rosalen, P. L., *Molecules* **2015**, *20*,  
2 7329-7358.  
3  
4 (8) Juergens, U. R.; Stöber, M.; Vetter, H., *Eur. J. Med.Res.* **1998**, *3*, 539-545.  
5  
6 (9) Kim, S.-H.; Lee, S.; Piccolo, S. R.; Allen-Brady, K.; Park, E.-J.; Chun, J. N.; Kim, T. W.; Cho,  
7 N.-H.; Kim, I.-G.; So, I.; Jeon, J.-H., *Biochem. Biophys. Res. Commun.* **2012**, *422*, 436-441.  
8  
9 (10) Li, Q.; Wang, X.; Yang, Z.; Wang, B.; Li, S., *Oncology* **2009**, *77*, 335-341.  
10  
11 (11) Kamatou, G. P. P.; Vermaak, I.; Viljoen, A. M.; Lawrence, B. M., *Phytochemistry* **2013**, *96*,  
12 15-25.  
13  
14 (12) Croteau, R. B.; Davis, E. M.; Ringer, K. L.; Wildung, M. R., *Naturwissenschaften* **2005**, *92*,  
15 562-577.  
16  
17 (13) Sell, C., *A fragrant introduction to terpenoid chemistry*. Royal Society of Chemistry:  
18 Cambridge, UK, 2003, p 43-64  
19  
20 (14) Pollack, R. M., *Bioorg. Chem.* **2004**, *32*, 341-353.  
21  
22 (15) Lange, B. M.; Mahmoud, S. S.; Wildung, M. R.; Turner, G. W.; Davis, E. M.; Lange, I.;  
23 Baker, R. C.; Boydston, R. A.; Croteau, R. B., *Proc. Natl. Acad. Sci. U. S. A.* **2011**, *108*, 16944-  
24 16949.  
25  
26 (16) Lange, B. M.; Mahmoud, S. S.; Wildung, M. R.; Turner, G. W.; Davis, E. M.; Lange, I.;  
27 Baker, R. C.; Boydston, R. A.; Croteau, R. B., *Proc. Natl. Acad. Sci. USA* **2011**, *108*, 16944-16949.  
28  
29 (17) Lawrence, B. M., *Mint: The genus Mentha*. Hardman, R., Ed. CRC Press, Boca Raton, FL,  
30 USA: 2007. p 1-547.  
31  
32 (18) Chemler, J. A.; Koffas, M. A., *Curr. Opin. Biotechnol.* **2008**, *19*, 597-605.  
33  
34 (19) Mitchell, W., *Curr. Opin. Chem. Biol.* **2011**, *15*, 505-515.  
35  
36 (20) Ajikumar, P. K.; Xiao, W. H.; Tyo, K. E. J.; Wang, Y.; Simeon, F.; Leonard, E.; Mucha, O.;  
37 Phon, T. H.; Pfeifer, B.; Stephanopoulos, G., *Science* **2010**, *330*, 70-74.  
38  
39 (21) Friedman, D. C.; Ellington, A. D., *ACS Synth. Biol.* **2015**, *4*, 1053-1055.  
40  
41 (22) Winter, J. M.; Tang, Y., *Curr. Opin. Biotechnol.* **2012**, *23*, 736-743.  
42  
43 (23) Toogood, H. S.; Cheallaigh, A. N.; Tait, S.; Mansell, D. J.; Jervis, A.; Lygidakis, A.;  
44 Humphreys, L.; Takano, E.; Gardiner, J. M.; Scrutton, N. S., *ACS Synth. Biol.* **2015**, *4*, 1112-1123.  
45  
46 (24) Croteau, R.; Venkatachalam, K. V., *Arch. Biochem. Biophys.* **1986**, *249*, 306-315.  
47  
48 (25) Crowell, P. L.; Gould, M. N., *Crit. Rev. Oncog.* **1994**, *5*, 1-22.  
49  
50 (26) Kjonaas, R. B.; Venkatachalam, K. V.; Croteau, R., *Arch. Biochem. Biophys.* **1985**, *238*, 49-  
51 60.  
52  
53 (27) Lupien, S.; Karp, F.; Wildung, M.; Croteau, R., *Arch. Biochem. Biophys.* **1999**, *368*, 181-192.  
54  
55 (28) Ringer, K. L.; Davis, E. M.; Croteau, R., *Plant Physiol.* **2005**, *137*, 863-872.  
56  
57  
58  
59  
60

- 1 (29) Ringer, K. L.; McConkey, M. E.; Davis, E. M.; Rushing, G. W.; Croteau, R., *Arch. Biochem.*  
2 *Biophys.* **2003**, *418*, 80-92.
- 3  
4 (30) Wüst, M.; Little, D. B.; Schalk, M.; Croteau, R., *Arch. Biochem. Biophys.* **2001**, *387*, 125-  
5 136.
- 6  
7 (31) Duetz, W. A.; Bouwmeester, H.; Beilen, J. B. v.; Witholt, B., *Appl. Microbiol. Biotechnol.*  
8 **2003**, *61*, 269-277.
- 9  
10 (32) Vining, K. J.; Johnson, S. R.; Ahkami, A.; Lange, I.; Parrish, A. N.; Trapp, S. C.; Vroteau, R.  
11 B.; Straub, S. C. K.; Pandelova, I.; Lange, B. M., *Mol. Plant* **2017**, *10*, 323-339.
- 12  
13 (33) Ha, N.-C.; Choi, G.; Choi, K. Y.; Oh, B.-H., *Curr. Opin. Struct. Biol.* **2001**, *11*, 674-678.
- 14  
15 (34) Kim, S. W.; Cha, S.-S.; Cho, H.-S.; Kim, J.-S.; Ha, N.-C.; Cho, M.-J.; Joo, S.; Kim, K. K.;  
16 Choi, K. Y.; Oh, B.-H., *Biochemistry* **1997**, *36*, 14030-14036.
- 17  
18 (35) Swainston, N.; Currin, A.; Day, P. J.; Kell, D. B., *Nucleic Acids Res.* **2014**, *42*, W395–W400.
- 19  
20 (36) Swainston, N.; Currin, A.; Green, L.; Breitling, R.; Day, P. J.; Kell, D. B., *PeerJ Comput. Sci.*  
21 **2017**, *3*, e120;DOI 10.7717/peerj-cs.120
- 22  
23 (37) Currin, A.; Swainston, N.; Day, P. J.; Kell, D. B., *Protein Eng., Des. Sel.* **2014**, *27*, 273–280.
- 24  
25 (38) Currin, A.; Swainston, N.; Day, P. J.; Kell, D. B., *Methods Mol. Biol. (N. Y., NY, U. S.)* **2017**,  
26 *1472*, 63–78.
- 27  
28 (39) Perrin, S.; Gilliland, G., *Nucleic Acids Res.* **1990**, *18*, 7433-7438.
- 29  
30 (40) Ke, S. H.; Madison, E. L., *Nucleic Acids Res.* **1997**, *25*, 3371-3372.
- 31  
32 (41) Ní Cheallaigh, A.; Mansell, D.; Toogood, H.; Tait, S.; Lygidakis, A.; Scrutton, N.; Gardiner,  
33 J., *Submitted*
- 34  
35 (42) Pedrioli, P. G. A.; Eng, J. K.; Hubley, R.; Vogelzang, M.; Deutsch, E. W.; Raught, B.; Pratt,  
36 B.; Nilsson, E.; Angeletti, R. H.; Apweiler, R.; Cheung, K.; Costello, C. E.; Hermjakob, H.; Huang,  
37 S.; Julian, R. K.; Kapp, E.; McComb, M. E.; Oliver, S. G.; Omenn, G.; Paton, N. W.; Simpson, R.;  
38 Smith, R.; Taylor, C. F.; Zhu, W.; Aebersold, R., *Nat. Biotechnol.* **2004**, *22*, 1459–1466.
- 39  
40 (43) Chambers, M. C.; Maclean, B.; Burke, R.; Amodei, D.; Ruderman, D. L.; Neumann, S.;  
41 Gatto, L.; Fischer, B.; Pratt, B.; Egertson, J.; Hoff, K.; Kessner, D.; Tasman, N.; Shulman, N.;  
42 Frewen, B.; Baker, T. A.; Brusniak, M.-Y.; Paulse, C.; Creasy, D.; Flashner, L.; Kani, K.;  
43 Moulding, C.; Seymour, S. L.; Nuwaysir, L. M.; Lefebvre, B.; Kuhlmann, F.; Roark, J.; Rainer, P.;  
44 Detlev, S.; Hemenway, T.; Huhmer, A.; Langridge, J.; Connolly, B.; Chadick, T.; Holly, K.; Eckels,  
45 J.; Deutsch, E. W.; Moritz, R. L.; Katz, J. E.; Agus, D. B.; MacCoss, M.; Tabb, D. L.; Mallick, P.,  
46 *Nat. Biotechnol.* **2012**, *30*, 918–920.
- 47  
48 (44) Winter, G.; Lobley, C. M.; Prince, S. M., *Acta Crystallogr., Sect. D: Biol. Crystallogr.* **2013**,  
49 *69*, 1260-73.
- 50  
51  
52  
53  
54  
55  
56  
57  
58  
59  
60

1 (45) McCoy, A. J.; Grosse-Kunstleve, R. W.; Adams, P. D.; Winn, M. D.; Storoni, L. C.; Read, R.  
2 J., *J. Appl. Crystallogr.* **2007**, *40*, 658-674.

3 (46) Adams, P. D.; Afonine, P. V.; Bunkoczi, G.; Chen, V. B.; Davis, I. W.; Echols, N.; Headd, J.  
4 J.; Hung, L. W.; Kapral, G. J.; Grosse-Kunstleve, R. W.; McCoy, A. J.; Moriarty, N. W.; Oeffner,  
5 R.; Read, R. J.; Richardson, D. C.; Richardson, J. S.; Terwilliger, T. C.; Zwart, P. H., *Acta*  
6 *Crystallogr., Sect. D: Biol. Crystallogr.* **2010**, *66*, 213-221.

7 (47) Emsley, P.; Lohkamp, B.; Scott, W. G.; Cowtan, K., *Acta Crystallogr., Sect. D: Biol.*  
8 *Crystallogr.* **2010**, *66*, 486-501.

9 (48) Afonine, P. V.; Grosse-Kunstleve, R. W.; Echols, N.; Headd, J. J.; Moriarty, N. W.;  
10 Mustyakimov, M.; Terwilliger, T. C.; Urzhumtsev, A.; Zwart, P. H.; Adams, P. D., *Acta*  
11 *Crystallogr., Sect. D: Biol. Crystallogr.* **2012**, *68*, 352-367.

12 (49) Frisch, M. J.; Trucks, G. W.; Schlegel, H. B.; Scuseria, G. E.; Robb, M. A.; Cheeseman, J.  
13 R.; Scalmani, G.; Barone, V.; Petersson, G. A.; Nakatsuji, H.; Li, X.; Caricato, M.; Marenich, A.;  
14 Bloino, J.; Janesko, B. G.; Gomperts, R.; Mennucci, B.; Hratchian, H. P.; Ortiz, J. V.; Izmaylov, A.  
15 F.; Sonnenberg, J. L.; Williams-Young, D.; Ding, F.; Lipparini, F.; Egidi, F.; Goings, J.; Peng, B.;  
16 Petrone, A.; Henderson, T.; Ranasinghe, D.; Zakrzewski, V. G.; Gao, J.; Rega, N.; Zheng, G.;  
17 Liang, W.; Hada, M.; Ehara, M.; Toyota, K.; Fukuda, R.; Hasegawa, J.; Ishida, M.; Nakajima, T.;  
18 Honda, Y.; Kitao, O.; Nakai, H.; Vreven, T.; Throssell, K.; J. A. Montgomery, J.; Peralta, J. E.;  
19 Ogliaro, F.; Bearpark, M.; Heyd, J. J.; Brothers, E.; Kudin, K. N.; Staroverov, V. N.; Keith, T.;  
20 Kobayashi, R.; Normand, J.; Raghavachari, K.; Rendell, A.; Burant, J. C.; Lyengar, S. S.; Tomasi,  
21 J.; Cossi, M.; Millam, J. M.; Klene, M.; Adamo, C.; Cammi, R.; Ochterski, J. W.; Martin, R. L.;  
22 Morokuma, K.; Farkas, O.; Foresman, J. B.; Fox, D. J. *Gaussian 09 D.01*, Gaussian, Inc.:  
23 Wallingford, CT, 2016.

24 (50) Becke, A. D., *J. Chem. Phys.* **1993**, *98*, 5648-5652.

25 (51) Grimme, S.; Antony, J.; Ehrlich, S.; Krieg, H., *J. Chem. Phys.* **2010**, *132*, 154104.

26 (52) Oostenbrink, C.; Villa, A.; Mark, A. E.; Van Gunsteren, W. F., *J. Comput. Chem.* **2004**, *25*,  
27 1656-1676.

28 (53) Van Der Spoel, D.; Lindahl, E.; Hess, B.; Groenhof, G.; Mark, A. E.; Berendsen, H. J. C., *J.*  
29 *Comput. Chem.* **2005**, *26*, 1701-1718.

30 (54) Ha, N. C.; Choi, G.; Choi, K. Y.; Oh, B. H., *Curr. Opin. Struct. Biol.* **2001**, *11*, 674-678.

31 (55) Schwans, J. P.; Kraut, D. A.; Herschlag, D., *Proc. Natl. Acad. Sci. U. S. A.* **2009**, *106*, 14271-  
32 14275.

33 (56) Mansell, D. J.; Toogood, H. S.; Waller, J.; Hughes, J. M. X.; Levy, C. W.; Gardiner, J. M.;  
34 Scrutton, N. S., *ACS Catal.* **2013**, *3*, 370-379.

1 (57) Siedenburg, G.; Jendrossek, D.; Breuer, M.; Juhl, B.; Pleiss, J.; Seitz, M.; Klebensberger, J.;  
2 Hauer, B., *Appl. Environ. Microbiol.* **2012**, *78*, 1055-1062.

3  
4 (58) Lygidakis, A.; Karuppiah, V.; Hoeven, R.; Ni Cheallaigh, A.; Leys, D.; Gardiner, J. M.;  
5 Toogood, H. S.; Scrutton, N. S., *Angew. Chem., Int. Ed. Engl.* **2016**, *55*, 9596-9600.

6 (59) Salis, H. M.; Mirsky, E. A.; Voigt, C. A., *Nat. Biotechnol.* **2009**, *27*, 946–950.

7 (60) Salis, H. M., *Methods Enzymol.* **2011**, *498*, 19-42.

8 (61) Alonso-Gutierrez, J.; Chan, R.; Batth, T. S.; Adams, P. D.; Keasling, J. D.; Petzold, C. J.;  
9 Lee, T. S., *Metab. Eng.* **2013**, *19*, 33–41.